Available online at www.sciencedirect.com
SCIENCE DIRECT
ELSEVIER
Journal of the European Ceramic Society 26 (2006) 2205–2212
ECERS
www.elsevier.com/locate/jeurceramsoc

Nickel–alumina graded coatings obtained by dipping and EPD on nickel substrates

Begoña Ferrari *, A. Javier Sánchez-Herencia, Rodrigo Moreno

Instituto de Cerámica y Vidrio, CSIC, Campus de Cantoblanco, c/Kelsen 5, E-28049 Madrid, Spain

Received 22 January 2005; received in revised form 30 March 2005; accepted 9 April 2005
Available online 1 June 2005

Abstract

Nickel substrates have been coated by Ni/Al_2O_3 composite films by a dipping process using aqueous suspensions that contain a temporary binder. Two-layer and three-layer graded coatings have been produced, consisting of pure Ni powder and Ni/Al_2O_3 composites with Al_2O_3 contents of 15 and 30 vol.% as intermediate layers to release sintering and thermal stresses. The laminates were further coated with a ceramic layer of Al_2O_3/ZrO_2 that was deposited by electrophoretic deposition using a non-aqueous suspension. A continuous, thin Al_2O_3 layer surrounding Ni grains developed at the intermediate composite layer of Ni/Al_2O_3 allows the ceramic coating to maintain strongly adhered to the nickel substrate by means of a porous substrate/coating interface.

Keywords: Shaping; Suspensions; Films; Composites; Ni/Al_2O_3

1. Introduction

The use of metals is limited in aggressive media or in high temperature applications, where metal undergoes corrosion and degradation. Ceramic coatings are often used to improve the surface behavior of metals, thus allowing them to be used in high temperature applications, such as thermal barrier coatings. One of the most widely studied metal–ceramic systems is the $Ni–Al_2O_3$ system,[1–3] due to the high refractoriness and stability of nickel. The incorporation of a ductile phase of Ni into an Al_2O_3 matrix has demonstrated to be an efficient route for improving the toughness of the ceramic phase.[4–6] Reinforcement occurs by means of a crack bridging mechanism, but its efficiency depends on the bonding characteristics, since defects at the interface, such as pores or unjoined areas may be the origin of damage and cracks induced by differences in thermal expansion coefficients. A lot of work has been made to obtain bulk $Ni–Al_2O_3$ bodies, but the application of this system to films and coatings have been much less studied.

A major problem when trying to join a ceramic layer and a metal one arises from their very different thermal expansion coefficients, leading to very high residual stresses on cooling.[7] Excepting some chemical processing routes, such as sol–gel,[8] ceramic powder processing usually requires high temperatures for sintering. Moreover, when a dense substrate is coated by a powdered layer, the former has no dimensional changes while the last shrinks on sintering, thus promoting new stresses.[9] Some of these problems have been solved using processing strategies to obtain defect-free bulk bodies. One such approach is to formulate compositions that develop a thermally-grown oxide (TGO) layer during the thermal treatment or pre-treatment. A film of ceramic-metal composite is formed that allows joining to both the ceramic and the metal layers giving consistency to the coating.[10,11] This intermediate layer reduces mismatch between the thermal expansion coefficients and thus, residual stresses. However, the mismatch between a porous layer that shrinks during sintering and a dense substrate remains unsolved.

For this problem the functionally graded material (FGM) concept is a very useful design tool. It was developed as a way to face the very high residual stresses developed in composites for aerospace applications. A FGM implies a grad-

* Corresponding author. Tel.: +34 91 7355840; fax: +34 91 7355843.
E-mail address: bferrari@icv.csic.es (B. Ferrari).

0955-2219/$ – see front matter © 2005 Elsevier Ltd. All rights reserved.
doi:10.1016/j.jeurceramsoc.2005.04.009

ual change in the composition from one face to another that allows the properties to progressively change inside the material. In this way, pure Ni to pure Al_2O_3 graded materials have been fabricated in one-step sintering by fixing the linear shrinkage of the composite layers forming the FGM.[12] Other method to coat metals with a ceramic phase is the electrochemical deposition of an intermediate metal layer prior to the coating forming[13] or once the coating has been formed through the channels of the presintered porous ceramic layer.[14]

Previous work has studied the colloidal behavior of nickel aqueous suspensions, demonstrating that well-dispersed suspensions can be prepared in water by using an acrylic-based polyelectrolyte and tetramethylammonium hydroxide at pH 10.[15] Other authors have studied also the stability and rheological properties of nickel suspensions.[16,17] We have also reported previously the use of nickel aqueous suspensions to produce thick coatings on the internal walls of steel tubes.[18] The suspension wetted to the steel by action of organic binders similar to those used for tape casting.

The present work deals with the manufacture of a graded microstructure in which a Ni foil is coated by Ni and Ni/Al_2O_3 layers prepared from aqueous suspensions with an organic binder and further deposition by dipping. Behind the metal–ceramic layers introduced to improve adhesion, an outer ceramic layer of Al_2O_3/ZrO_2 is formed by electrophoretic deposition.

2. Experimental

Commercial powders of Nickel (T110, INCO, Canada), ZrO_2 with 3 mol% Y_2O_3 (TZ-3YS, Tosoh, Japan), and α-Al_2O_3 (Condea, HPA05, USA) with mean particle sizes of 2.5, 0.4 and 0.35 μm, specific surface areas of 1.0, 6.7 and 9.5 $m^2\,g^{-1}$, and densities of 8.7, 5.8 and 3.95 $g\,cm^{-3}$, respectively, were used.

Aqueous suspensions of Ni (100N) and Ni/Al_2O_3 mixtures with relative ratios of 85/15 and 70/30 (v/v) (labeled as 15A and 30A, respectively) were prepared to final solids contents of 20, 25 and 30 vol.% (after binders addition). According to previous studies[15] suspensions were stabilized with a commercial polyacrylic acid based polyelectrolyte (Duramax D-3005, Rohm and Haas, USA) adding tetramethyl ammonium hydroxide (TMAH) up to pH 10. Polyelectrolyte concentration was 0.8 wt.% with regard to Al_2O_3 and 1 wt.% with regard to Ni. Suspensions were prepared by ultrasonic mixing using a 400 W sonication probe (IKA U400S, Germany) for 2 min and further stirring for 1 h.

Slurries for dipping were prepared adding 10 wt.% of a commercial acrylic emulsion (Mowilith DM765, Celanese Emulsions, Spain). The suspensions flow behaviour was measured with a rheometer RS50 (Haake, Germany) operating at controlled shear rate conditions ranging from 0 to 1500 s^{-1}. The sensor system consisted of a double-cone rotor and a stationary plate, protected with a solvent trap to reduce evaporation.

Commercially available foils of pure nickel were used as coating substrates. Single coatings of 100N, 15A and 30A were obtained by dipping at a withdrawal rate of 7.5 mm s^{-1}. Two-layer (2L) coatings were prepared by sequentially dipping into suspensions 100N and 30A. Three-layer (3L) coatings were obtained by consecutive immersion into 100N, 15A and 30A suspensions. Coatings are labeled as 2L-20%, 3L-25%, etc, where 2L and 3L refer to the number of layers and the percentage number refers to the solids loading of the used suspensions. Every formed layer was weighted after 24 h drying to calculate the deposited mass/unit area.

The 100N, 2L and 3L coatings were further coated with an external ceramic layer of Al_2O_3/ZrO_2 (relative ratio of 65.45/34.55, v/v) by electrophoretic co-deposition. The A/Z suspension was prepared to a solids content of 3.4 vol.% in ethanol by dispersing with 0.4 wt.% of polyethyleneimine (PEI, Aldrich). A graphite foil was used as counterelectrode, separated at a distance of 2 cm from the work electrode. A constant current density of 50 $\mu A\,cm^{-2}$ was applied for a deposition time of 90 s, using a power source AMEL, mod. 551 (UK). EPD equipment was provided with a lift in order to assure a constant withdrawal rate of 7.5 mm s^{-1}.

Dynamic sintering tests were recorded on bulk pieces obtained from suspensions of each composition with a dilatometer (Netzsch, Germany) up to 1450 °C in flowing N_2 atmosphere. Samples were thermally treated in N_2 atmosphere at 1450 °C for 3 h, with heating rates of 5 °C min^{-1} and cooling rates of 2 °C min^{-1}, and a dwell at 500 °C for 30 min during heating, to allow de-binding. Microstructural observations and thickness measurements were made by scanning electron microscopy (SEM, Zeiss DSM-400, Germany).

3. Results and discussion

3.1. Monolithic dip-coatings

The flow behavior of 100N, 15A and 30A suspensions with solids contents of 20, 25, and 30 vol.% was measured at controlled rate conditions. All suspensions exhibit a shear-thinning behavior, in agreement with that reported before for nickel slurries.[19] The shear-thinning behavior increases with the addition of 10 wt.% of binder, which improves the adhesion of the coatings produced by dipping.

Fig. 1 shows the values of viscosity measured at 100 s^{-1} and the weight/unit area of the dip-coatings deposited on the nickel substrates from suspensions with different composition as a function of their solids loadings. The plot evidences that viscosity increases with the solids concentration and decreases with increasing concentration of Al_2O_3. The increase of viscosity leads to an increase of the deposited mass, as it is clearly observed for suspension 100N, although for 30 vol.% composite suspensions (15A and 30A) the deposited mass is lower than expected.

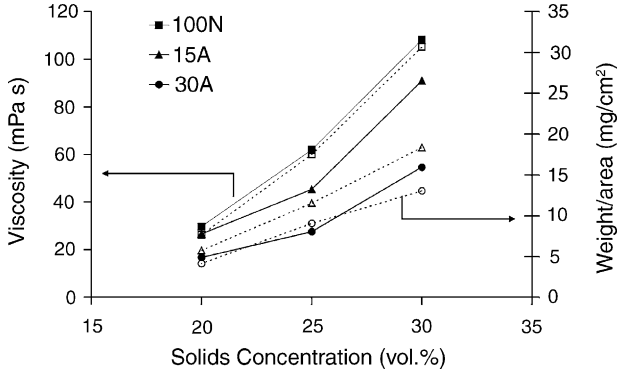

Fig. 1. Viscosity (continuous lines) of 100N, 15A, and 30A suspensions and weight/unit area of the resulting dry dip-coatings (dashed lines).

Monolithic coatings 15A and 30A were prepared by dipping and sintered at 1450 °C for 3 h. Both coatings maintain firmly joined to the nickel substrate, without releasing when pulling out with scotch tape. Ni powders were also deposited by dipping, acting as a substrate for subsequent deposition of the multiple layers.

Deposited Ni films have a green thickness ranging from 25 to 100 μm, while that of A15 and A30 coatings range from 12 to 50 μm, depending on the solids content of the suspension. Table 1 relates the viscosity of the suspensions with the deposited mass and the green and sintered thickness. Summarized results show that the higher is the viscosity the greater is the thickness. Furthermore, the relative green density of the deposited films tends to increase as the content of alumina increases. The Ni coatings have the lowest packing density, due to the larger particle size of Ni powders. The addition of submicronic alumina leads to a bimodal size distribution that improves particles packing.

Fig. 2 shows SEM micrographs of 15A sintered coatings obtained from suspensions with solids contents of 20 (a), 25 (b) and 30 vol.% (c). All the coatings are characterized by a porous Ni matrix joined to the substrate, the largest porosity appearing at the interface. Small grains of Al_2O_3 are found either inside the Ni grains, especially for 25 and 30 vol.% coatings, or at the surface. It appears that both the density and the thickness uniformity increase with increasing solids contents.

In agreement with Table 1, the increase of the viscosity values of the suspensions versus the solids content promotes a thickness increase, and also higher densification, since solvent evaporation is the only mechanism operating during shaping.

Fig. 3 shows a SEM micrograph of a 30A coating, obtained from suspensions with 20 vol.% solids. Isolated coarse grains of nickel are surrounded by the finer Al_2O_3 grains but the joining between substrate and coating is quite poor, and cracking occurs at the interface.

For dynamic sintering studies bulk monoliths were obtained by pouring suspensions of every composition with a solids content of 20 vol.% into non-porous steel molds. Fig. 4a shows the shrinkage curves of samples 100N, 15A, 30A, and A/Z. The corresponding derivative curves are plotted in Fig. 4b. Nickel shows a first shrinkage stage at 550 °C that has been previously assigned[19] to the formation of necks between fine particles, and a second stage with a change of slope at 900 °C, corresponding to the maximum sintering rate (Fig. 4b). The final shrinkage of the samples is around 30%. For the sample 15A, the slope of the shrinkage curve decreases, and the first peak in the derivative shifts up to above 700 °C, as the introduction of Al_2O_3 retards sintering. In the derivative two further peaks appear centered at 900° and 1150 °C. The sintering rate coincides with that of pure nickel at around 850 °C. Shrinkage increases at temperatures above 1400 °C, as the ceramic phase has not fully densified. When increasing the amount of alumina (sample A30) the shrinkage is seriously reduced, since the concentration of second phase is large enough to difficult continuous contact between nickel particles. In the case of the A/Z sample, shrinkage starts at 1200 °C. At the final temperature of this experiment (1450 °C) no full densification has been reached but the sintering process has achieved the maximum shrinkage rate indicating that a dwell at this temperature will increase the final density of this layer.

According to these studies it can be predicted that a multilayer composed of 100N–A15N and/or A30N can be used to join the ceramic layer (A/Z) to a dense metallic sub-

Table 1
Suspensions and coatings properties

Composition	Solids content (vol.%)	Viscosity (mPa s)	Weight/area (±0.2 mg/cm²)	Thickness	
				Green (±5 μm)	Sintered (±1 μm)
100N	20	30	8	26	–
	25	62	18	56	–
	30	108	31	102	–
15A	20	27	6	18	10
	25	45	11	40	17
	30	91	18	53	22
30A	20	17	4	12	8
	25	28	9	30	16
	30	55	13	35	–

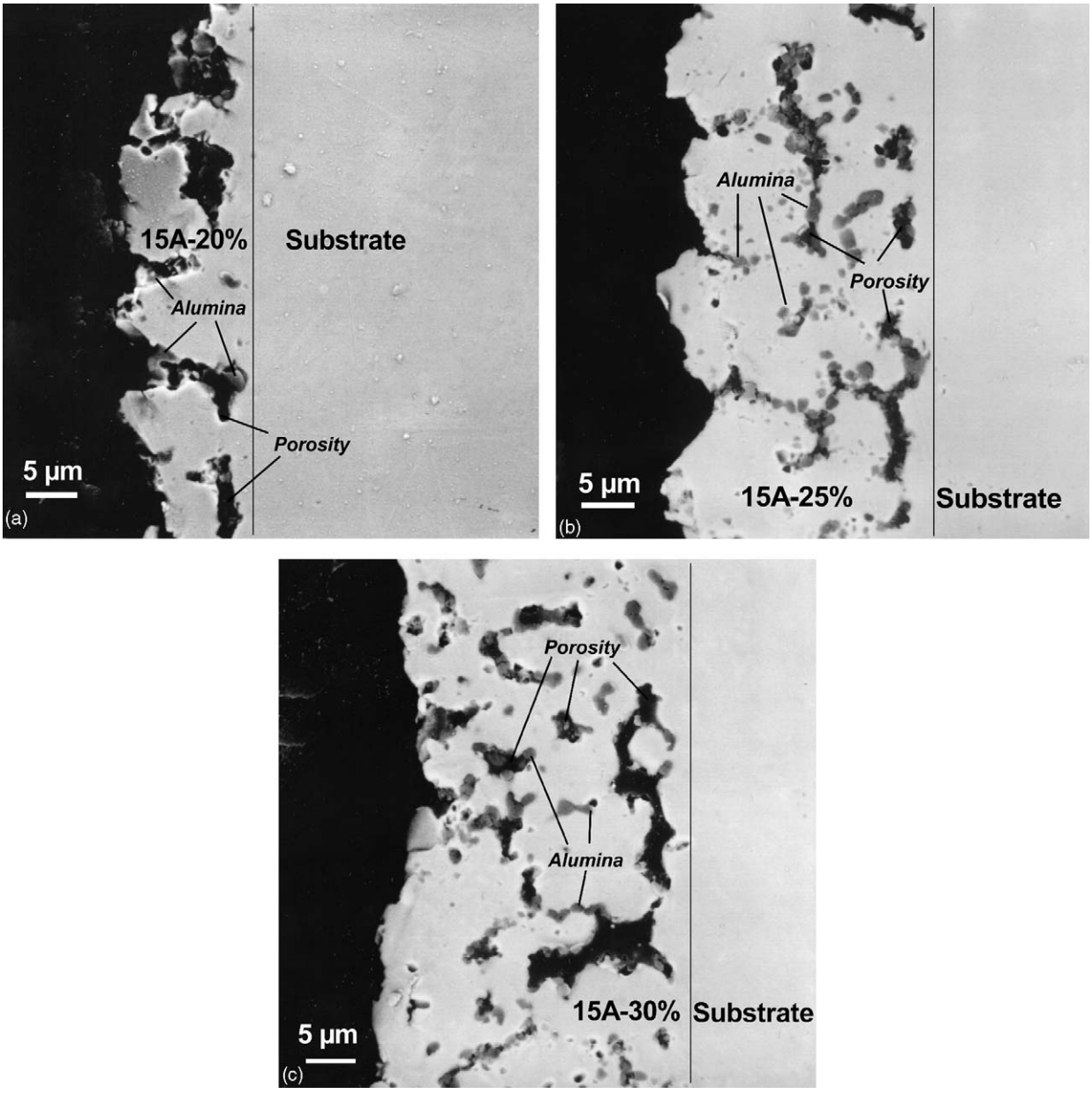

Fig. 2. SEM microstructures of 15A coatings obtained from suspensions with solids loadings of 20 (a), 25 (b), and 30 (c) vol.%.

strate. As the temperature achieves 550 °C the nickel and the metal–ceramic layers start to form necks and slight shrinkage takes place. At 900 °C the nickel and nickel–alumina layers should be joined to the nickel substrate. At this temperature nickel has reached the maximum shrinkage rate but this is not the case of nickel–alumina layers, which need higher temperatures. As can be seen in Fig. 4a the shrinkage of the different layers develops a stepwise system that will match the sintering stresses generated by the adjacent layer and no delamination would occur. It has to be noted that dilatometric studies have been performed on monolithic samples with the same composition as that of the layers, but the final shrinkage and sintering rate will be different in a layered coating.[9]

3.2. Multilayer coatings

Table 2 summarizes the sequence of layers in the multilayer coatings fabricated by sequential dipping from suspensions of different solids contents. Dipping, and not elec-

Table 2
Sequence of layers in the multilayer coatings

Suspension solids content (vol.%)	Layers sequence	
	2L (100N–30A) (%)	3L (100N–15A–30A) (%)
20	2L-20	3L-20
25	2L-25	3L-25
30	2L-30	3L-30

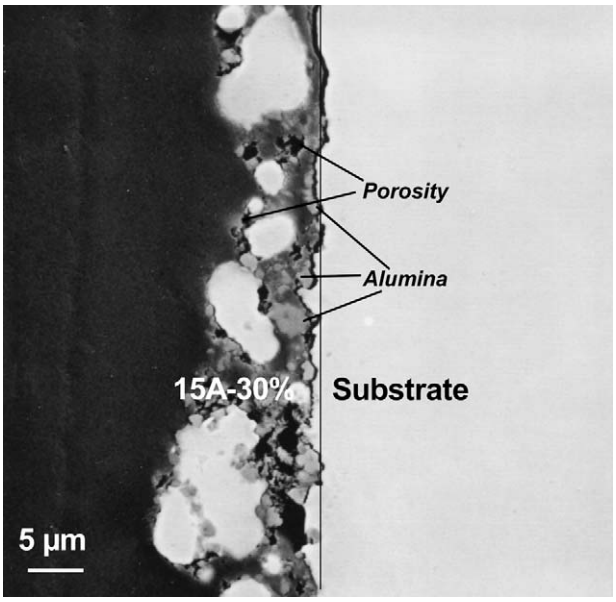

Fig. 3. SEM microstructures of 30A coating obtained from suspensions with 20 vol.% solids.

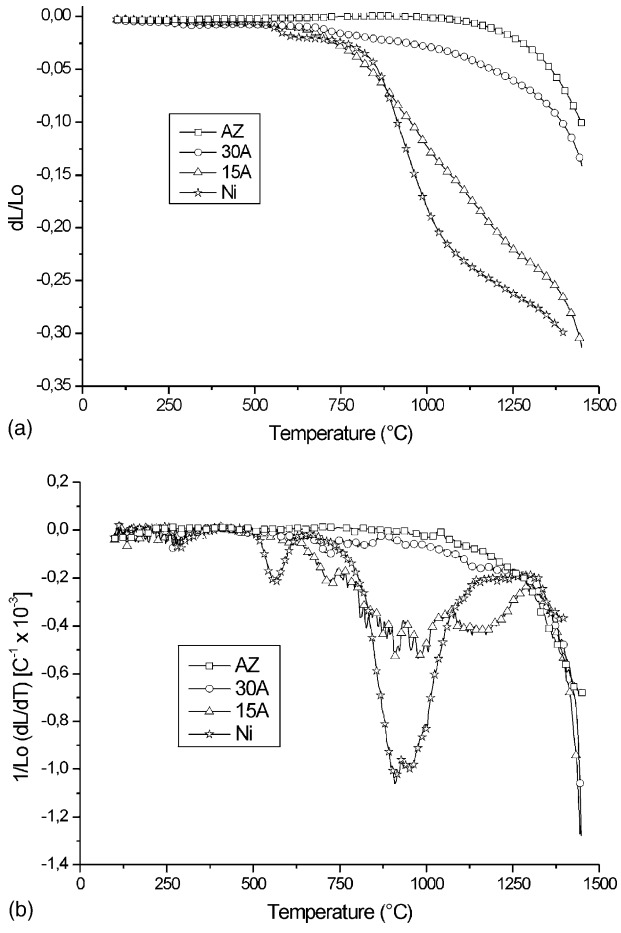

Fig. 4. Dynamic sintering curves of the monoliths: (a) linear shrinkage, $\Delta L/L_0$, vs. temperature and (b) linear shrinkage rate, $d(\Delta L/L_0)/dT$, vs. temperature.

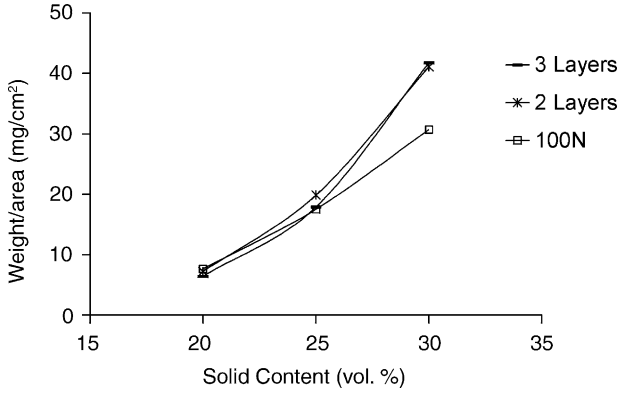

Fig. 5. Deposited mass of 100N, 2L, and 3L coatings as a function of the solids content of suspensions.

trophoresis, was selected to shape intermediate layers in order to reduce the thickness of the gradient structure.

Fig. 5 shows the weight/unit area of the coatings with two and three layers (2L and 3L) compared to that obtained for 100N (1L), versus the solids content. The total deposited weight in 2L and 3L coatings using 20 and 25 vol.% suspensions is similar to that of the first layer (100N), thus meaning that these layers are very thin. However, when using 30 vol.% suspensions, there is a significant contribution of the ceramic-containing layers to the total mass of the deposit. Results point out that multi-step dipping does not increase the deposits weight as it would be expected. Deposited layers characterized in Table 1 were shaped on the nickel foil while sequential deposits were shaped on the film of Ni powders deposited before. The lower deposit weight is due to the different nature of the substrate surface.

Ceramic coatings of alumina–zirconia (A/Z) were deposited by EPD, using as work electrodes the nickel substrates with single coating (100N), 2L coating (100N–30A), and 3L coating (100N–15A–30A). The mass/unit area of the A/Z coating ranged from 11 to 18 mg cm^{-2}. Deposits are slightly heavier when deposition is performed directly on the 100N layer, regardless of the solids content, which suggests that there is other process involved in the deposit formation different to the electrophoresis. Other authors suggest the possible existence of an additional contribution to the deposit growth due to the solvent filtration on a porous substrate.[20] The 100N green structure is more porous than 15A and 30A structures, so the filtration effect during electrophoresis may be significant.

Multilayer coatings were thermally treated at 1450 °C in N_2 atmosphere. A/Z layers partially released on sintering when directly deposited on 100N coatings, but when 15A and/or 30A layers are present the A/Z layer maintained adhered to the substrate. Apparently, no differences between 2L and 3L coatings were observed at the interface. Ceramic layers only showed external cracks at the edges, due to increased thickness close to the substrate edges under the effect of the electric field during EPD.

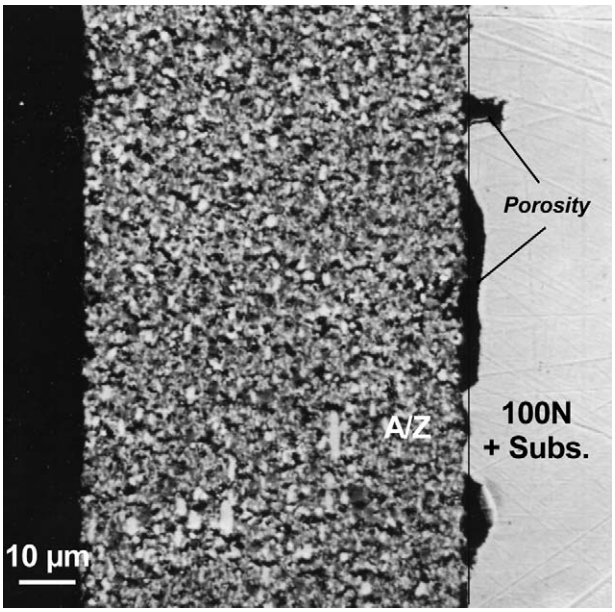

Fig. 6. SEM microstructure of Al_2O_3/ZrO_2 layer deposited by EPD on the 100N–20% layer.

Microstructural observations by SEM show that the thickness of the A/Z layers ranges from 40 to 50 μm, the thicker being those deposited onto 100N coatings, in good agreement with the weight/unit area measurements. Multilayer coating composed by a 100N-20% (without alumina) and the outer A/Z layer (Fig. 6) shows that the nickel 100N layer joins to the nickel substrate with no residual porosity or defects at the interface, but the joining between the deposited nickel layer and the ceramic layer is worst, probably due to the shrinkage mismatch.

SEM pictures of Fig. 7 show a general view (a) and a detail (b) of the multilayer 3L-20% coated by A/Z layer. The Ni layer has joined to the substrate, as well as to the 15A layer, although some pores appear aligned at the interface between nickel layer and substrate, in contrast with the microstructure observed in Fig. 6. The A15N and A30N layers have mixed and cannot be well differentiated. Large grains of nickel are surrounded by fine alumina particles and a relatively large porosity remains. This structure is 20 μm thick, and it seems that Al_2O_3 content increases toward the ceramic layer.

In the case of the 2L intermediate coating, the outer ceramic layer also adhered to the substrate after sintering. Microstructures in Fig. 8 show multilayer coatings with intermediate layers 2L-25% (a) and 2L-20% (b). In both cases the Al_2O_3/Ni layer is thinner than that developed with the 3L-20% multilayer system (Fig. 7). Its thickness increases with the solids content from 5 to 10 μm. Isolated pores appear in the 2L-25% microstructure (Fig. 8a) at the interface between nickel layer and substrate, whereas the 2L-20% material has no residual porosity and the powdered Ni layer cannot be distinguished from the Ni substrate. Although the second layer

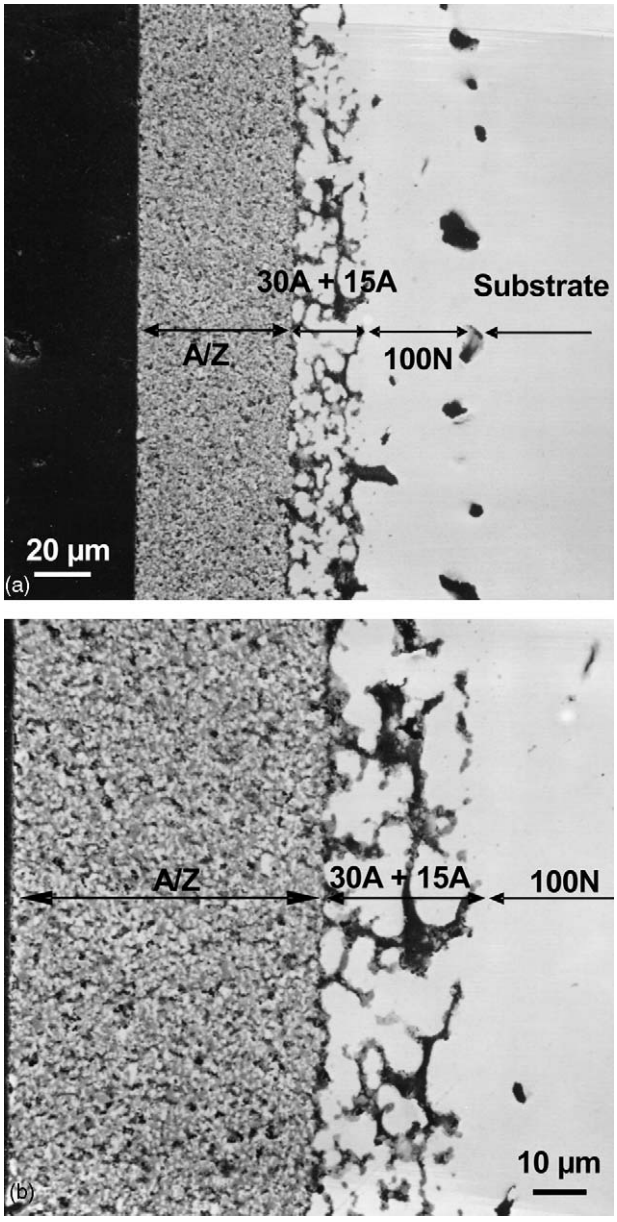

Fig. 7. SEM microstructure of the multilayer 3L-20% coated by Al_2O_3/ZrO_2 EPD layer, at two different magnifications.

in 2L-25% system (Fig. 8a) has similar composition to the last layer of 3L-20% system (Fig. 7b), the anchoring of Ni grains of the composite layer to the pure Ni layer seems to be stronger, showing a closer structure. This effect can be also observed in the 2L-20% multilayer.

In summary, a metal–ceramic composite with graded structure has been formed by means of intermediate porous layers that adsorb stresses occurring during sintering. Juncture regions increase with both the solids content (8a, 8b) and the number of layers (7b, 8b). The adhesion of the coating to the Ni sheet is strongly improved when a thin layer of Ni powders is deposited on the Ni foil. An external dense layer of Al_2O_3-ZrO_2 up to 50 μm in thickness

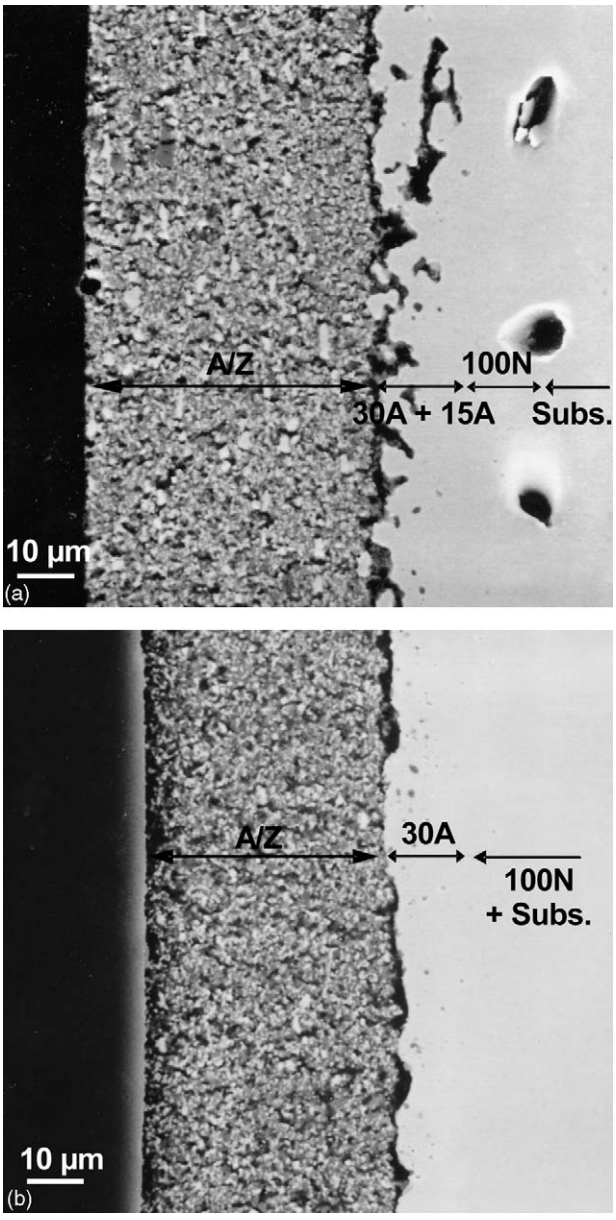

Fig. 8. SEM microstructure of the multilayers 2L-25% (a) and 2L-20% (b), both coated by an Al_2O_3/ZrO_2 EPD layer.

can be deposited by electrophoresis on the metal–ceramic layer.

4. Conclusions

A functionally graded coating shaped by dipping has been designed to join a metal substrate to a thick ceramic layer (up to 50 μm), the last being deposited by an electrophoresis process. Multilayer system is constituted by two clearly differentiated layers: a Ni layer that uniformly joins to the Ni substrate, and a composite Al_2O_3/Ni layer after a thermal treatment at 1450 °C (5–20 μm). While Ni grains at the composite layer join to the Ni layer, the development of a continuous, thin Al_2O_3 layer (<1 μm) surrounding the Ni grains promotes the joining of this layer to the A/Z deposit. Shaping conditions (sequence of layers, solids concentrations and composition of the suspensions) will be optimized in further works to remove the isolated pores appearing at the interface between the deposited nickel layer and the substrate.

Acknowledgements

This work has been supported by CICYT, Spain (contract MAT 2003-836). Dr. Ferrari acknowledges CSIC and European Social Foundation for their financial support.

References

1. Trumble, K. P. and Rühle, M., The thermodynamics of spinel interphase formation at diffusion-bonded Ni/Al_2O_3 interfaces. *Acta Metall. Mater.*, 1991, **39**(8), 1915–1924.
2. Sekino, T., Nakajima, T., Ueda, S. and Nihara, K., Reduction and sintering of a nickel-dispersed-alumina composite and its properties. *J. Am. Ceram. Soc.*, 1997, **80**(5), 1139–1148.
3. Tuan, W. H. and Brook, R. J., The toughening of alumina with nickel inclusions. *J. Eur. Ceram. Soc.*, 1990, **6**(1), 31–37.
4. Tuan, W. H. and Brook, R. J., Processing of alumina/nickel composites. *J. Eur. Ceram. Soc.*, 1992, **10**(2), 95–100.
5. Lourdin, P., Juvé, D. and Tréheux, D., Nickel–alumina bonds: mechanical properties related to interfacial chemistry. *J. Eur. Ceram. Soc.*, 1996, **16**(7), 745–752.
6. Chang, L., Chen, S. C., Tuan, W. H. and Brook, R. J., Interfacial characterization of Al_2O_3-Ni composites. *J. Eur. Ceram. Soc.*, 1993, **12**(6), 479–485.
7. Bao, G. and Cai, H., Delamination cracking in functionally graded coating/metal substrate systems. *Acta Mater.*, 1997, **45**(3), 1055–1066.
8. Castro, Y., Ferrari, B., Moreno, R. and Durán, A., Silica sol–gel coatings on metals produced by EPD. *J. Sol–Gel Sci. Technol.*, 2003, **26**(1–3), 735–739.
9. Bordia, R. K. and Raj, R., Sintering behavior of ceramic films constrained by a rigid substrate. *J. Am. Ceram. Soc.*, 1985, **68**(6), 287–292.
10. Wang, Z., Shemilt, J. and Xiao, P., Fabrication of ceramic composite coatings using electrophoretic deposition, reaction bonding and low temperature sintering. *J. Eur. Ceram. Soc.*, 2002, **22**(2), 183–189.
11. Wang, X. and Xiao, P., Residual stresses and constrained sintering of YSZ/Al_2O_3 composite coatings. *Acta Mater.*, 2004, **52**(9), 2591–2603.
12. Winter, A. N., Corff, B. A., Reimanis, I. E. and Rabin, B. H., Fabrication of graded nickel–alumina composites with a thermal-behavior-matching process. *J. Am. Ceram. Soc.*, 2000, **83**(9), 2147–2154.
13. Wang, Z., Xiao, P. and Shemilt, J., Fabrication of composite coatings using a combination of electrochemical methods and reaction bonding process. *J. Eur. Ceram. Soc.*, 2000, **20**(10), 1469–1473.
14. Kruger, H. G., Knote, A., Schindler, U., Kern, H. and Boccaccini, A. R., Composite ceramic-metal coatings by means of combined electrophoretic deposition and galvanic methods. *J. Mater. Sci.*, 2004, **39**(3), 834–839.
15. Hernández, N., Sánchez-Herencia, A. J., Moreno, R. and Fierro, J. L. G., Surface behaviour of Ni powders in aqueous suspensions. *J. Phys. Chem. B*, 2005, **109**(10), 4470–4474.
16. Tseng, W. J. and Chen, C. N., Determination of maximum solids concentration in nickel nanoparticle suspensions. *J. Mater. Sci. Lett.*, 2002, **21**(5), 419–422.

17. Tseng, W. J. and Chen, C. N., Effect of polymeric dispersant on rheological behavior of nickel–terpineol suspensions. *Mater. Sci. Eng. A*, 2003, **347**, 145–153.
18. Ferrari, B., Sánchez-Herencia, A. J. and Moreno, R., Porous nickel coatings on steel tubes formed by aqueous colloidal processing. *Adv. Eng. Mater.*, 2002, **4**(9), 690–694.
19. Sánchez-Herencia, A. J., Millán, A. J., Nieto, M. I. and Moreno, R., Aqueous colloidal processing of nickel powder. *Acta Mater.*, 2001, **49**(4), 645–651.
20. Bieshemel, P. M. and Verweij, H., Theory of cast formation in electrophoretic deposition. *J. Am. Ceram. Soc.*, 1999, **82**(6), 1451–1455.